January 15, 2007

# Multiplex Biosensor Using Gold Nanorods

Chenxu Yu, *Purdue University*
Joseph Irudayaraj, *Purdue University*

*Anal. Chem.* **2007,** *79,* 572−579

# Multiplex Biosensor Using Gold Nanorods

**Chenxu Yu and Joseph Irudayaraj**

*Department of Agricultural and Biological Engineering and Bindley Biosciences Center, Purdue University, 225 South University Street, West Lafayette, Indiana 47907*

**Gold nanorods (GNRs) with different aspect ratios were fabricated through seed-mediated growth and surface activation by alkanethiols for the attachment of antibodies to yield gold nanorod molecular probes (GNrMPs). Multiplex sensing was demonstrated by the distinct response of the plasmon spectra of the GNrMPs to binding events of three targets (goat anti-human IgG1 Fab, rabbit anti-mouse IgG1 Fab, rabbit anti-sheep IgG (H+L)). Plasmonic sensors are highly specific and sensitive and can be used to monitor refractive index changes caused by molecular interactions in their immediate vicinity with potential to achieve single-particle biosensing. This technique can play a key role in developing novel optical biosensors for both in vivo and in vitro detection and single-receptor kinetics.**

Gold nanoparticles (GNRs) possess optical properties that make them uniquely suitable for biosensing applications. Their optical properties strongly depend on both the particle size and shape and are related to the interaction between the metal conduction electrons and the electric field component of the incident electromagnetic radiation, which leads to strong, characteristic absorption bands in the visible to infrared part of the spectrum.[1]

In aqueous solutions, gold nanostructures exhibit strong plasmon bands depending on their geometric shape and size. For spherical particles, a strong absorption band around 520 nm due to the excitation of plasmons by incident light can be readily observed.[1] For nanorods, two distinct plasmon bands, one associated with the transverse (~520 nm) mode and the other with the longitudinal mode (usually >600 nm), could be observed.[1] Plasmon modes have also been reported for more complex structures such as prisms and quadrupoles.[2] Applications[3−11] based on wavelength shifts due to changes in dielectric properties in the vicinity of the particles (known as nanoSPR,[3] or localized surface plasmon resonance[4]) achieved by connecting biological receptor molecules (i.e., antibodies) to activated gold nanoparticles with a compatible chemical tether exists. The subsequent interaction of these gold nanoparticle-based molecular probes to their corresponding targets (antigens) completes the sensing modality.

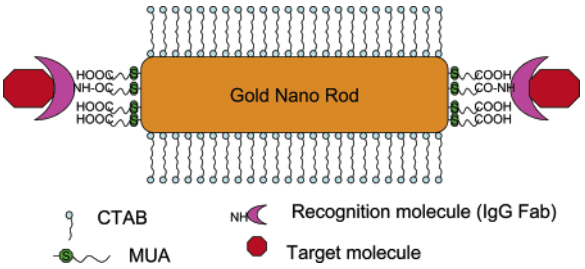


**Figure 1.** Schematic illustration of a gold nanorod molecular probe.

Most of the existing work utilizing the nanoSPR mechanism was based on binding-induced aggregation of spherical particles. The concept here is that, when the separation distance between particles is comparable to or smaller than their radii, the oscillation of the plasmons from adjacent particles can become coupled, lowering their vibration frequency that appear as absorption bands red-shifted to longer wavelengths. The red-shift is dependent upon the number of particles and their spatial arrangement within the aggregate.[12] A 50−100-nm red-shift with a significant broadening of the absorption bands due to overlapping of shifted modes of vibration was observed.[3] Mirkin and co-workers used gold nanoparticles to develop a one-pot colorimetric sensor for DNA detection utilizing the aggregation of DNA-capped gold nanospheres due to DNA hybridization and reported a sharp melting transition capable of detecting insertions, deletion, and mismatches at a single-base resolution.[13−15] Lee and Perez-Luna[11] constructed epoxy-functionalized gold nanospheres through a series of steps to subsequently react with hydroxyl moieties of the α-D-glucopyranosyl groups of carboxylated dextran chain. The interaction of this material with three proteins was then investigated through changes in the plasmon spectra of gold nanoparticles. This work

* To whom all correspondence should be addressed. E-mail: josephi@purdue.edu.

(1) Perez-Juste, J.; Pastoriza-Santos, I.; Liz-Marz'an, L. M.; Mulvaney, P. *Coord. Chem. Rev.* **2005**, *249*, 1870−1901.
(2) Millstone, J. E.; Park, S.; Shuford, K.; Qin, L.; Schatz, G. C.; Mirkin, C. A. *J. Am. Chem. Soc.* **2005**, *127*, 5312−5313.
(3) Nath, N.; Chilkoti, A. *J. Fluoresc.* **2004**, *14*, 377−389.
(4) Haes, A.; van Duyne, R. P. *J. Am. Chem. Soc.* **2002**, *124*,10596−10604.
(5) Nath, N.; Chilkoti, A. *Anal. Chem.* **2002**, *74*, 504−509.
(6) Yonzon, C. R.; Jeoung, E.; Zou, S.; Schatz, G. C.; Mrksich, M.; Van Duyne, R. P. *J. Am. Chem. Soc.* **2004**, *126*, 12669−12676.
(7) Ghosh, S. K.; Nath, S.; Kundu, S.; Esumi, K.; Pal, T. *J. Phys. Chem. B* **2004**, *108*, 13963−13971.
(8) Dahlin, A.; Zach, M.; Rindzevicius, T.; Kall, M.; Sutherland, D. S.; Hook, F. *J. Am. Chem. Soc.* **2005**, *127*, 5043−5048.
(9) Raschke, G.; Kowarik, S.; Franzl, T.; Sonnichscen, C.; Klar, T. A.; Feldmann, J.; Nichtl, A.; Kurzinger, K. *Nano Lett.* **2003**, *3*, 935−938.
(10) Raschke, G.; Brogl, S.; Susha, A. S.; Rogach, A. L.; Klar, T. A.; Feldmann, J.; Fieres, B.; Petkov, N.; Bein, T.; Nichtl, A.; Kurzinger, K. *Nano Lett.* **2004**, *4*, 1853−1857.
(11) Lee, S.; Perez-Luna, H. *Anal. Chem.* **2005**, *77*, 7204−7211.
(12) Quinten, M.; Kreibig, U. *Surf. Sci.* **1986**, *172*, 557−577.
(13) Elghanian, R.; Storhoff, J. J.; Mucic, R. C.; Letsinger, R. L.; Mirkin, C. A. *Science* **1997**, *277*, 1078−1081.
(14) Jin, R.; Wu, G.; Li, Z.; Mirkin, C. A.; Schatz, G. C. *J. Am. Chem. Soc.* **2003**, *125*, 1643−1654.
(15) Taton, T. A.; Mirkin, C. A.; Letsinger, R. L. *Science* **2000**, *289*, 1757−1760.



10.1021/ac061730d CCC: $37.00 
Published on Web 12/16/2006

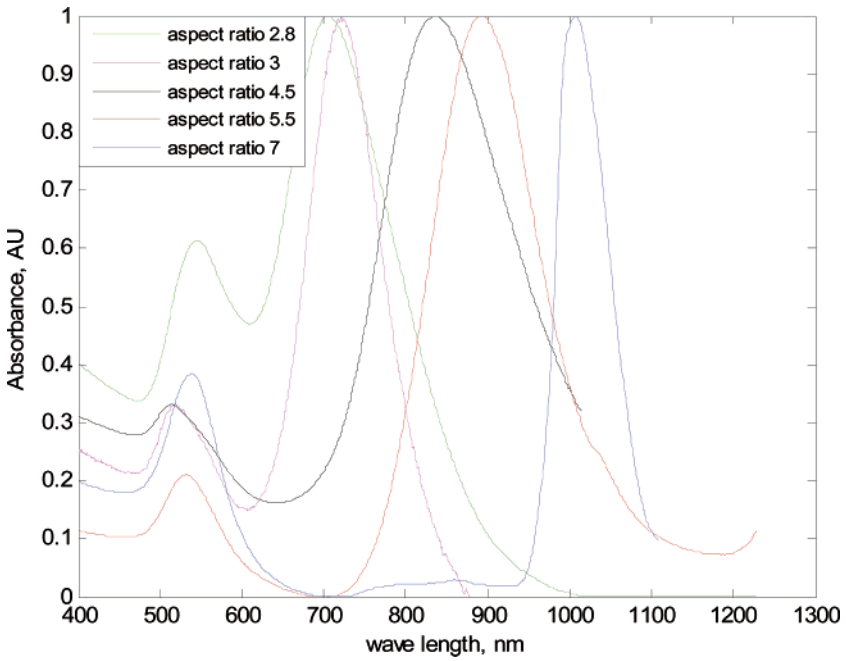


**Figure 2.** Absorption spectra of gold nanorods with different aspect ratios.

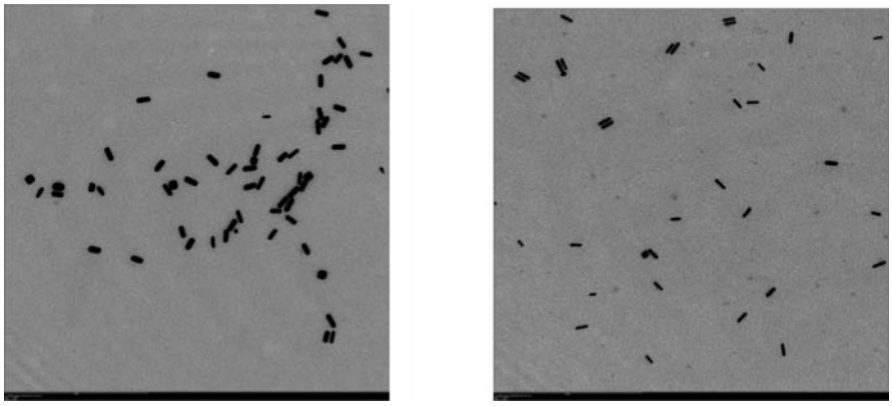

**Figure 3.** TEM micrographs of gold nanorods with mean aspect ratios 2.8 and 4.5.

revealed that the binding of these proteins is concentration-dependent over a wide range (~100 nM to 50 $\mu$M), and a simple and convenient colorimetric method to monitor biospecific interactions was suggested.

The refractive index-dependent plasmon spectral peak shift of nonaggregated spherical gold nanoparticles was also used to develop a solution-phase immunoassay to monitor the binding kinetics of antibody−antigen interactions in real time.[16,17] Monoclonal antibodies specific to human ferritin, human chorionic gonadotropin, and human heart fatty acid binding protein functionalized to gold particles gave rise to a red-shift in the SPR extinction resulting in an increase in the extinction intensity at 600 nm upon binding to the target. The assay was performed in an automated clinical analyzer offering tremendous potential for high sample throughput.

There are two ways to evaluate changes in the plasmon spectra caused by target binding: wavelength change of the plasmon peak or extinction/absorption intensity change at a fixed wavelength (i.e., 600 nm). When spherical particles coated with Fab segments of monoclonal antibodies specific to a single epitope on the ligand were constructed, aggregation was not observed.[17] Since the wavelength shift of the plasmon peak was only 2~3 nm (also observed in our own experiments), which is too small a value for detection purposes (low signal/noise ratio), the latter (intensity change at 600 nm) was often used as an indicator of target binding events. However, this approach has an inherent problem: the change in extinction intensity could also occur due to a change in particle concentration. When multiple washing steps are incorporated to remove unbound analytes in a "lab-in-a-tube" setup (in some of the one-pot colorimetric study proposed earlier), uncertain changes in the nanoparticle concentration can occur and contribute to the "noise" component of extinction intensity changes, thus making it difficult to monitor biospecific interactions events.

Observation of the wavelength shift of the plasmon bands on the other hand is solely determined by changes in the dielectric properties (i.e., refractive indexes) in the immediate vicinity of the nanoparticles; concentration change has a minimal or no effect on this parameter. Hence the wavelength shift of the plasmon band

(16) Englebienne, P. *Analyst* **1998**, *123*, 1599−1603.
(17) Englebienne, P.; Van Hoonacker, A.; Valsamis, J. *Clin. Chem.* **2000**, *46*, 2000−2003.

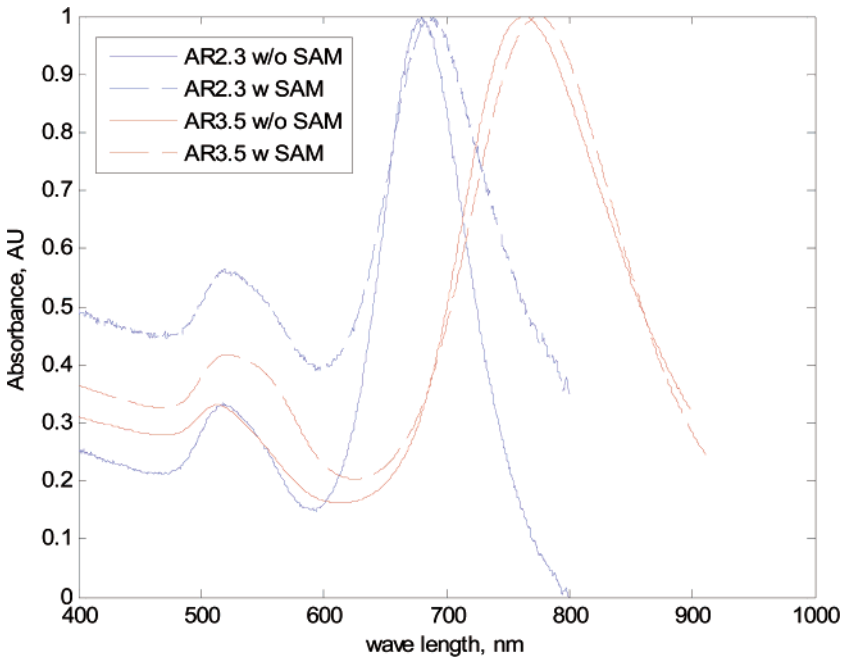


**Figure 4.** Plasmonic spectra of gold nanorods with AR = 2.3 and 3.5, before and after SAM formation.

**Table 1. Concentration of IgGs in the Supernatant (nmol/10 mL) after 1 h o Immobilization onto the Gold Nanorods (*n* = 3)**

| | GNrMP | | | |
|---|---|---|---|---|
| | aspect ratio 2.3 | aspect ratio 3.5 | aspect ratio 4.5 | aspect ratio 6.5 |
| IgG Fabs | 0.82 ± 0.08 | 0.90 ± 0.07 | 0.87 ± 0.08 | 0.85 ± 0.08 |
| binding ratio | 1.18 ± 0.08 | 1.1 ± 0.07 | 1.13 ± 0.08 | 1.15 ± 0.08 |

has a greater potential for biosensing. In order to induce a large enough shift for detection purposes, when spherical particles are used, the sensors are designed based on the controlled aggregation concept.[11,13−15] Since aggregation results in a large wavelength shift with a significant widening of the plasmon peak, the resulting spectral resolution is too poor to distinguish multiple targets or for specific detection purposes. Van Duyne and co-workers[6] demonstrated that anisotropic silver nanoparticles (tetrahedron) experienced a large shift in the plasmon maximum upon target binding without aggregation, and a microarray was constructed using these silver nanoparticles for molecular fingerprinting. We believe that gold nanorods can be used to overcome this "aggregation deficit" as effectively; furthermore, because gold nanorods with different aspect ratios could be easily fabricated, unique "multiplexing" advantage could be realized.

When anisotropic particles such as nanorods are used to create gold nanorod molecular probes (GNrMPs), single-particle sensors could be devised. Significant changes in the plasmon spectra in response to a change in the refractive index in the vicinity of GNrMPs could be observed and utilized to sense specific target-binding events, as illustrated in Figure 1. The longitudinal plasmon bands are extremely sensitive to changes in the dielectric properties of the surroundings, for example, for nanorods with an aspect ratio of 3 suspended in liquid matrix, a change in refractive index of 0.1 unit of the liquid matrix causes a red-shift of ~40 nm from the longitudinal plasmon band.[1] The sensitivity increases as the aspect ratio of the nanorods increases, as demonstrated by El Sayed and co-workers, both experimentally and theoretically.[18−20] Small changes in the aspect ratio can lead to drastic changes in the transmitted colors/plasmon spectra, suggesting significant multiplexing potential when carefully designed GNrMPs are deployed for simultaneous detection of multiple targets. In this work, we will demonstrate, for the first time, multiplex biosensing using GNrMPs, and the detection of target binding monitored via direct spectral changes induced by changes in refractive index in the vicinity of individual particles, not by aggregation/assembly of the nanoparticles.

GNRs fabricated through seed-mediated growth normally have CTAB caps preferentially attached to their {1,1,0} and {1,0,0} side faces. The attachment of CTAB to the {1,1,1} side faces is weaker and as such this face is more exposed and accessible to the chemical linkers.[21−23] There have been several reports in which alkanethiols are introduced onto the {1,1,1} side faces of gold nanorods, through hydrogen bonds between alkanethiol molecules[23] or through binding of biomolecules to the alkanethiol layer[21,22] to result in a head-to-tail chainlike formation of gold nanorod aggregates. In this study, a thiol functionalization procedure was utilized to selectively bind recognition agents to

(18) Lee, K. S.; El-Sayed, M. A. *J. Phys. Chem. B* **2006**, *110*, 19220−19225.
(19) Jain, P. K.; Eustis, S.; El-Sayed, M. A. *J. Phys. Chem. B* **2006**, *110*, 18243−18253.
(20) Link, S.; El-Sayed, M. A. *J. Phys. Chem. B* **2005**, *109*, 10531−10532.
(21) Chang, J.; Wu, H.; Chen, H.; Ling, Y.; Tan, W. *Chem. Commun.* **2005**, 1092−1094.
(22) Caswell, K. K.; Wilson, J. N.; Bunz, U. H. F.; Murphy, C. J. *J. Am. Chem. Soc.* **2003**, *125*, 13914−13915.
(23) Thomas, K. G.; Barazzouk, S.; Ipe, B. I.; Shibu, J. S. T.; Kamat, P. V. *J. Phys. Chem. B* **2004**, *108*, 13066−13068.

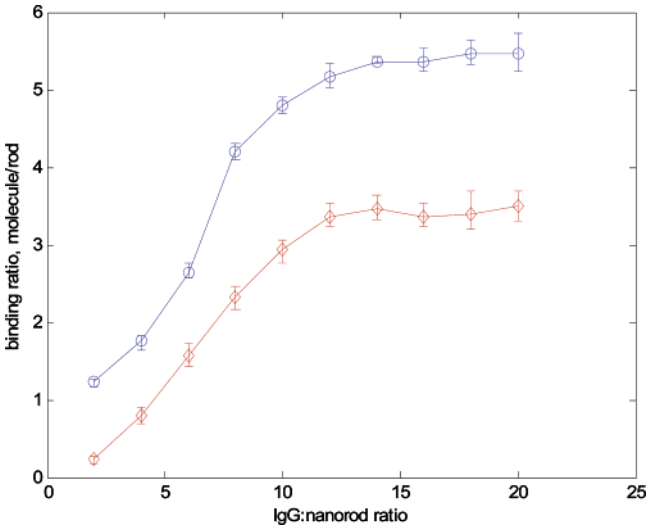


**Figure 5.** Functionalization efficiency of activated and nonactivated gold nanorods.

gold nanorods that can bind to their respective ligands for multiplex biosensing. Although recently gold nanorods have been investigated as possible bio/optical sensors that utilize the two-photon or three-photon excited luminescent emission,[24,25] using them as nanoSPR sensors for multiplexing purposes has not been demonstrated.

## EXPERIMENTAL SECTION

**Fabrication of Gold Nanorods.** A seed-mediated growth procedure slightly modified from that suggested by Nikoobakht and El-Sayed[26] was used to fabricate gold nanorods with aspect ratio between 2.5 and 7. Hexadecyltrimethylammoniumbromide ($C_{16}$TAB, 99%) and benzyldimethylammoniumchloride hydrate (BDAC, 99%), sodium borohydride (99%), L-ascorbic acid, gold-(III) chloride hydrate (>99%), and silver nitrate (>99%) were all purchased from Sigma-Aldrich (St. Louis, MO) and used without further purification. Nanopure deionized and distilled water (18.2 MΩ) was used for all experiments.

Nanorod fabrication was initiated by adding small gold particles as seeds (~4 nm) into aqueous solution containing the CTAB capping agent, gold ions (present in $HAuCl_4$), reducing agents (in ascorbic acid), and silver ions (in $AgNO_3$). By adjusting the concentrations of the chemicals in the solution, nanorods of different aspect ratios were fabricated. To synthesize nanorods with aspect ratios larger than 4.5, a two-surfactant system was used. Here, the seeds were grown in aqueous solution containing BDAC and CTAB at different ratios, gold ions, silver ions, and reducing agents. By adjusting the relative content of these ingredients, gold nanorods with aspect ratio up to 7 were fabricated.

The concentration of nanorods was estimated by measuring the average distance between adjacent particles present in the TEM images. At least 150~200 particles from each of the images were analyzed to yield a mean interparticle distance. It should be noticed that this estimation is rough and cannot be considered as an accurate indication of particle concentration.

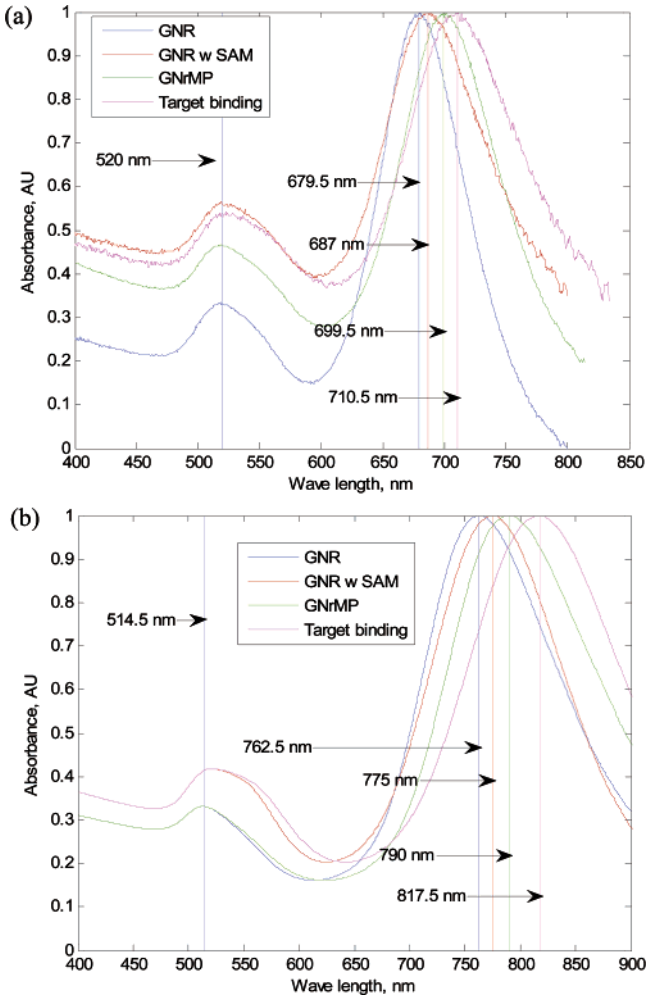


**Figure 6.** Detection of single epitope targets by GNrMPs. (a) GNrMP 1; (b) GNrMP2.

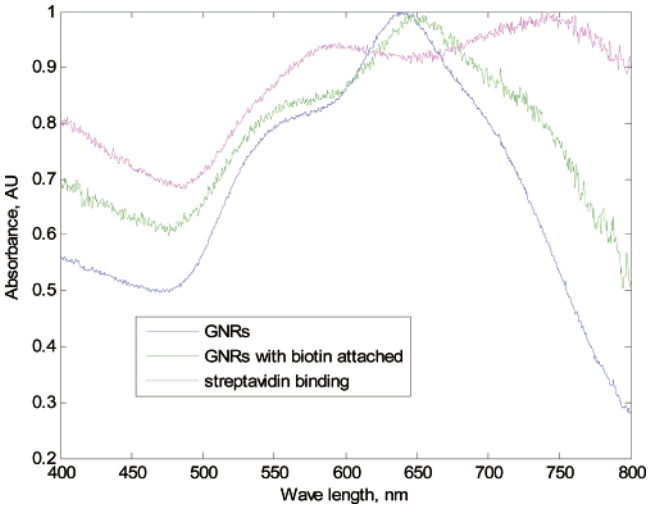


**Figure 7.** Head-to-tail aggregation caused by streptavidin binding to biotinylated GNRs.

The nanorod growth reaction was terminated after 3 h by removing the reaction solution by centrifugation at 5000 rpm for 15 min. Some small spherical particles were also removed since they were retained in the supernatant. The nanorods were

(24) Wang, H.; Huff, T. B.; Zweifel, D. A.; He, W.; Low, P. S.; Wei, A.; Cheng, J. X. *Proc. Natl. Acad. Sci. U.S.A.* **2005**, *102*, 15752−15756.
(25) Li, C.; Male, K. B.; Hrapovic, S.; Luong, J. H. T. *Chem. Commun.* **2005**, 3924−3926.
(26) Nikoobakht, B.; El-Sayed, M. A. *Chem. Mater.* **2003**, *15*,1957−1962.

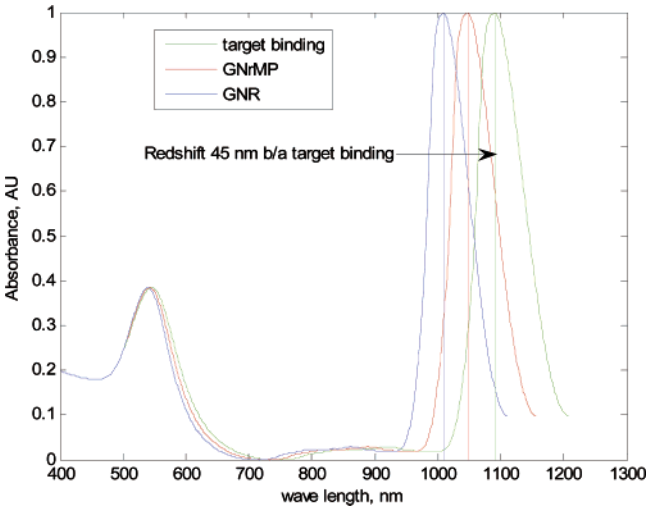


**Figure 8.** Detection of double-epitope targets by GNrMPs of aspect ratio 7.0.

resuspensed in 0.005 M CTAB solutions and found to remain stable for up to 100 days. All subsequent characterization, activation, and functionalization were conducted with these nanorod samples.

**Functionalization of Gold Nanorods To Make GNrMPs.** Once synthesized, the nanostructures can be functionalized by chemical and biological elements and deployed as sensors. Biofunctionalization constitutes a two-step process: in step 1, termed the activation step, a chemical anchor layer was formed on the nanorod surface to provide active functional groups to which biological molecules (i.e., antibodies) can be covalently attached; and in step 2, the functionalization step, biomolecules were covalently linked to the anchor layer to produce GNrMPs for target specific sensing.

Partial activation of the freshly made gold nanorods was done by incubating the nanorods with alkanethiol compounds to form an alkanethiol monolayer on the {1,1,1} side faces of the rod by self-assembly. Such a process will retain the CTAB capping at the {1,1,0}/{1,0,0} side faces. At the {1,1,1} side faces, the alkanethiol self-assembled monolayers (SAMs) was formed to present active groups (i.e., COOH) that can be used to tether antibodies through NH−CO bonds.

The chemical modification/activation of GNRs was achieved as follows: 11-mercaptoundecanoic acid (MUA) was purchased from Sigma-Aldrich; 0.5 mL of 20 mM ethanol solution of MUA was added into 5 mL of the gold nanorod solution and stirred mildly for 24 h under room temperature. Nanorods were then collected by centrifugation at 5000 rpm for 15 min and resuspended in a 0.005 M CTAB solution to yield a final concentration of ∼100 nM.

Once the MUA SAM was formed, Fab segments of human and mouse IgGs were then attached to the activated nanorods as follows: to 5 mL of the activated nanorods (∼100 nM), 1 mL of freshly prepared 0.4 M 1-ethyl,3-(3-dimethylaminopropyl) carbodiimide (Sigma-Aldrich) and 0.1 M 4-(4-maleimidophenyl)butyric acid *N*-succinimidyl ester (Sigma-Aldrich) solution was added and sonicated for 25 min at 4 °C. The resulting nanorods were then collected by centrifugation at 5000 rpm for 5 min and resuspended in a 5 mL of PBS buffer (pH 7.4) containing 0.005 M CTAB. IgG Fabs suspended in PBS were then added to the resulting nanorod suspension (the concentration of IgG Fab was ∼200 nM) and then incubated for 1 h under constant sonication at room temperature. The functionalized nanorods were subsequently collected by centrifugation at 5000 rpm for 5 min. After three rounds of vigorous washing, the collected nanorods were sonicated in 0.005 M CTAB solution for 10 min, the supernatant after each washing step was collected and added together, and the protein content of the combined supernatant was measured using a Bio-rad protein assay (Bio-rad Laboratories, Hercules, CA) with bovine serum albumin as a protein standard. The amount of IgGs bound to the nanorods was determined by subtracting the IgGs left in the supernatant from the original amount. A control experiment was conducted with nonactivated nanorods to evaluate the physisorption of IgGs to the CTAB capped side faces via electrostatic interaction.

**Characterization of the Gold Nanorods.** The yield and aspect ratios of the gold nanorods was determined using transmission electron microscopy (TEM), acquired with a Philips CM-100 TEM (Philips, Eindhoven, Netherlands) operating at 100 kV, 200-$\mu$m condenser aperture, 70-$\mu$m objective aperture, and a spot 3. TEM grids were prepared by placing 1 $\mu$L of the nanorod solution in a 400-mesh Formvar-coated copper grid and evaporating the solution at room temperature. Images were then captured using a Tietz F415 slow scan digital camera at 4K resolution. At least 150−200 nanorods could be counted and measured per grid to calculate the mean aspect ratio of the nanorods after the synthesis step.

Absorption spectra of GNrMP samples through each stage of experiments were measured using a Jasco V570 UV−visible−NIR spectrophotometer (Jasco, Inc., Easton, MD), in the wavelength range between 400 and 1500 nm. The measured spectra were normalized by rescaling the maximum absorbance of the longitudinal plasmon peak to 1.

## RESULTS AND DISCUSSION

**Nanorod Fabrication.** Gold nanorods of aspect ratios in the range between 2.8 and 7 were made following the single0 and double-surfactant protocols discussed earlier. Figure 2 shows the absorption spectra of nanorods with aspect ratios of 2.8, 3, 4.5, 5.5, and 7, respectively. It can be clearly seen that small changes in aspect ratio introduce a significant red-shift of the longitudinal plasmon band of the GNR colloids, implying a significant potential for multiplexing. Within the range of this study, a linear correlation could be established between the aspect ratio of gold nanorods and the absorbance wavelength of the longitudinal plasmon bands; hence, the aspect ratio of gold nanorods could be easily deduced from their plasmon spectra (data provided in Supporting Information). The concentrations of nanorods were estimated through TEM imaging. A droplet (1 $\mu$L) of the nanorod suspension was spread on a TEM grid for observation. The evaporation of water during sample drying pushes the nanorods toward the rim of grid and resulted in a more densely packed distribution of the nanorods in the TEM view field, and the observed interparticle distances tend to be smaller than the real values, which leads to a larger concentration value being calculated. Therefore, the concentration so estimated is indeed an upper limit of the real concentration of the nanorods; they were found to be quite consistent (∼25−30

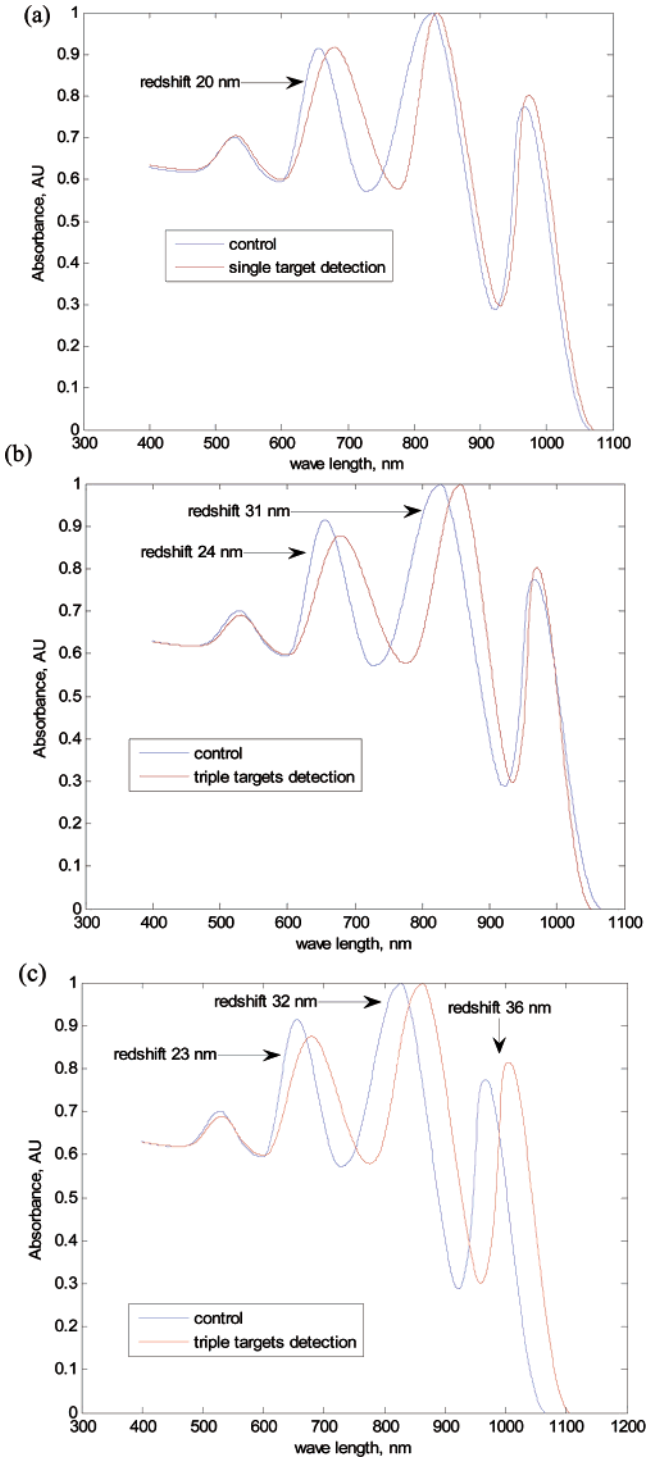


**Figure 9.** Multiplexing detection of various targets using GNrMPs. (a) One target; (b) two targets; (c) three targets.

nM) regardless of the aspect ratios of the nanorods as long as the quantity of seed used was constant.

Figure 3 shows TEM images of the nanorods of aspect ratios 3 and 4.5. Counting particles in the images taken for each type indicated that the final particles contain 95 and 96.5% rods, respectively, confirming the validity of the protocol. Another observation is that the width of the nanorods remained approximately the same; hence, an increase in aspect ratio was predominately determined by elongation of nanorods.

It should be noted that as the ratio reaches 7, the longitudinal peak red-shifts to ~1011 nm, well beyond the visible and into the NIR region of the spectrum where biological samples such as cells only have weak absorption and their interference with the plasmon signal is negligible (there is a weak and broad band ~800−1000 nm due to small amount of shorter rods, fragmented rods, and particles of other shapes, which is not important in the context of this work). Hence, these GNRs have a major advantage compared to the existing fluorescence and illumination labels where interferences due to sample autofluorescence could pose a significant problem in target detection.

**Functionalization of Gold Nanorods To Make GNrMPs.** Functionalization of gold nanorods takes advantage of the well-known affinity between gold and thiol compounds. However, because the {1,1,0}/{1,0,0} side faces of the rods are covered by CTAB, only the {1,1,1} side faces are easily utilized by alkanethiols to form SAMs, for attachment of recognition agents (antibodies in this work). It should, however, be noted that the formation of alkanethiol SAM introduces a red-shift of the plasmon peaks due to the changes in refractive index at the surface of the gold nanorods. Figure 4 shows the spectra of two types of nanorod (aspect ratios 2.3 and 3.5, respectively) suspensions before and after alkanethiol (MUA) attachment. A red-shift of 5−7 nm in the longitudinal peaks is clearly identifiable, indicating the alkanethiol SAM formation. Repeated measurement of spectra of the same nanorod sample over an elongated period of time (3 days) yields a maximum peak drift of 0.5 nm, toward both red and blue ends, showing that the 5−7-nm red-shift can only be caused by SAM formation.

Once the MUA SAM is formed, biomolecules can be covalently attached via the $NH_2$ bond of the antibodies to the COOH terminus of the MUA SAM. A further red-shift of the plasmon peak can be observed due to the antibody functionalization. The same two type of rods, after the human IgG Fab attachment, showed a significant shift (of up to 20 nm) compared to the unmodified rods (data provided in Supporting Informtion). The sensitivity of the plasmon spectra of the nanorods to the attachment of layers of molecules forms the basis of molecular biosensors using single particles.

If IgG Fabs only attach to MUA SAM at the {1,1,1} side faces, the number of IgG Fabs attached to each nanorod could be estimated. According to the TEM images, the edges of the nanorods with the {1,1,1} side faces have diameters ~7−10 nm and IgG Fabs are of cylindrical shape with a size of ~6 nm.[27] Therefore, under ideal conditions, two IgG Fabs can attach to each side of one gold nanorod and yield a 2:1 IgG Fab/rod ratio. From the length (~20−50 nm) and nanorod material stiffness, it could be reasoned that the IgG Fabs bound to the ends of a rod could only bind to different individual target molecules to provide a highly sensitive and specific platform.

Although IgGs can only covalently attach to the MUA-activated sites, physisorption of IgGs to the CTAB capped side faces is also possible. The isoelectric points for IgG Fabs are ~6;[28] hence, at a pH of ~7.4 during the functionalization reaction, the IgG Fabs are negatively charged, and they will bind to the positively charged CTAB cap via electrostatic interaction. However, physisorbed IgGs

(27) Kienberger, F.; Mueller, H.; Pastushenko, V.; Hingterdorfer, P. *EMBO Rep.* **2004**, *5*, 579−583.
(28) Bremer, M. B.; Duval, J.; Norde, W.; Lyklema, J. *Colloids Surf., A* **2004**, *250*, 29−42.

**Table 2. GNrMP/Target Pairs Investigated in Detection Experiments**

| GNrMP | no. 1 | no. 2 | no. 3 |
|---|---|---|---|
| GNR aspect ratio | 2.1 | 4.5 | 6.5 |
| recognition agent of GNrMPs | monoclonal human IgG1 Fab | monoclonal mouse IgG1 Fab | monoclonal sheep IgG (H+L) |
| target | monoclonal goat anti-human IgG Fab | monoclonal rabbit anti-mouse IgG Fab | monoclonal rabbit anti-sheep IgG (H+L) |

are not as strongly attached to the GNrMP surfaces as covalently bound ones; under vigorous washing after functionalization, a significant portion of these would be removed. In order to obtain GNrMPs that have consistent IgG coating, the MUA activation route is preferred, especially when a low IgG/nanorod ratio is used.

Table 1 provided a binding ratio of the IgGs to four different gold nanorods determined by measuring the remaining IgG contents in the supernatant after the functionalized GNrMPs were collected by centrifugation. The binding ratio here is defined as the average number of IgG molecules attached to each individual gold nanorod. For the concentration ratio used in our experiment (IgG Fab:gold nanorod = 2:1), if only covalent binding occurs, under a coupling efficiency of 100%, this binding ratio would be close to 2. However, in reality, the binding ratio appears to be not very high (~1.18) and rather independent of the aspect ratio of the GNRs; roughly 1 IgG Fab molecule/gold nanorod is obtained.

A separate experiment was conducted to investigate the effect of increased IgG concentrations on the functionalization of the nanorods (aspect ratio 2.1, 100 nM). As the IgG/nanorod ratio increases from 2:1 to 20:1, the binding ratio increases from 1.2 to 5.5 and levels off, as shown in Figure 5. Also it is observed that, at low IgG/nanorod ratio, the binding ratio of IgGs to activated gold nanorods is quite low (~0.2). Binding to activated nanorods is consistently higher than to nonactivated rods; at high IgG/nanorod ratio, on average two more IgG Fab molecules are bound to each nanorod, due to the covalent binding to the MUA-activated sites. Nevertheless, the GNrMPs used for target detection in this work had a binding ratio of ~1.2, so a 1:1 binding to target molecules was expected. Whether or not the IgG Fab is covalently bound to the MUA-activated site is not of critical importance.

**Detection of Biological Targets Using GNrMPs.** GNrMPs were made using human IgG Fab and gold nanorods of aspect ratio 2.3 (GNrMP 1) and gold nanorods of aspect ratio 3.5 (GNrMP 2). It has been reported that a head-to-tail aggregation of gold nanorods could be realized when two nanorods are connected by binding to the same ligand (for example, a biotin−streptavidin binding). If the ligand has only one active binding site to which the GNrMP can interact, head-to-tail aggregation will not occur and the plasmon spectral changes observed will be due to binding events from individual GNrMPs.

Figure 6 depicts the detection of goat anti-human IgG Fabs using GNrMP 1 and 2 via successive plasmon shifts. The plasmon peaks near 520 nm are not very sensitive to the refractive index change induced by target binding, and the red-shifts of these peaks are below 3 nm, thus offering no opportunity for the detection of specific target binding. The longitudinal peaks of the nanorods are extremely sensitive to the refractive index changes induced by target binding, suggesting that they are excellent reporters of target specific binding events and have the potential to achieve single-molecule sensitivity if measured using microspectroscopy. The sensitivity of the longitudinal peaks to the refractive index changes in their vicinity increases significantly with the aspect ratio of the rods, a red-shift of 11 and 27.5 nm is observed due to target binding to GNrMP 1 and 2 with aspect ratios of 2.3 and 3.5, respectively.

In order to ensure that the plasmon spectral changes observed are not due to head-to-tail aggregation, a comparison study was done using the biotin−streptavidin model as the recognition−target pair. Earlier work[13] has reported an expected head-to-tail aggregation of streptavidin with partially biotinylated gold nanorods,[18] because of the four active biotin-binding sites of the streptavidin molecules. As shown in Figure 7, the longitudinal peak of gold nanorods (aspect ratio 2.0) experienced a small red-shift after partial biotinylation and a subsequent red-shift of ~100 nm together with significant band-broadening after 20 $\mu$g/mL streptavidin was added to the solution, which could primarily be due to significant aggregation of the nanorods. Further, the transverse peak experienced a ~40-nm red-shift as well. Thus, we conclude that significant aggregation introduces a large red-shift in both the transverse and longitudinal bands together with significant band-broadening. Comparing the characteristics of Figures 4 and 7, it is obvious that the plasmon shifts observed in Figure 4 are not due to aggregation.

A head-to-tail aggregation of gold nanorods requires multiple epitopes in the targets (to serve as ligand bridges) oriented favorably for simultaneous head-to-tail coupling. Whole IgG molecules have two antigen-binding sites; however, if the targets are also immunoglobulins, the Y-shape of the two molecules will introduce a spatial hindrance that would render the head-to-tail connection of the molecules an unfavorable process. Thus, even if whole IgG molecules (2 binding sites) are used as targets instead of IgG Fabs (1 binding site), aggregation should not be significant and the single-particle-based target detection scheme proposed should be possible. Figure 8 shows the results obtained with a GNrMPs (aspect ratio of 7) containing a monoclonal sheep IgG whole molecule as a probe agent binding to a rabbit anti-sheep IgG whole molecule target. Clearly, aggregation is not a dominant phenomenon in this illustration.

The main advantage of GNrMPs is the multiplexing potential offered by the aspect ratio dependence of the wavelength of the longitudinal bands. To this date, this advantage has not been fully utilized. To demonstrate multiplex detection of various targets, a system using three GNrMP−target pairs was constructed (Table 2). A 3-mL aliquot of a mixture of an equal amount of each of the three GNrMPs was placed in three separate test tubes, and an equal amount (1 mL at 20 $\mu$g/mL) of sample 1 (containing target 1), sample 2 (a mix of target 1 and target 2), or sample 3 (a mix of target 1, target 2, and target 3) was separately added and the

resultant mixture incubated for 30 min under sonication at room temperature. The solution was then centrifuged at 3500 rpm for 5 min, the supernatant was discarded, the GNrMPs were resuspended in PBS buffer containing 0.005 M CTAB and the plasmon spectra measured are shown in Figure 9.

When sample 1 was added, the GNrMP tagged with the respective probe specifically interacted with this target to present a significant red-shift of up to 20 nm due to its longitudinal plasmon peak; the other two GNrMPs experienced a smaller red-shift in their respective longitudinal plasmon bands due to nonspecific binding, but these red-shifts were below 5 nm and can be easily distinguished from the well-defined red-shift due to target specific binding. When test sample 2 was added, the two peaks associated with the respective GNrMPs containing the probes experienced significant red-shifts of 24 and 31 nm, respectively. When all the three targets were added, the three longitudinal peaks showed a red-shift, indicating specific target-binding events. The red-shift increased as the aspect ratio of the GNrMPs increased, thus accomplishing multiplexing sensing of up to three targets in one test tube.

The probe−target systems used in our experiments are not inherently highly specific. For instance, mouse IgGs bind to rabbit anti-mouse IgG with high affinity; however, due to molecular homology, mouse IgGs will have some binding toward the other two targets, goat anti human IgGs and rabbit anti sheep IgGs, with a low but nonzero affinity. This is the origin of the nonspecific binding signals observed in the multiplexing detection scheme. It is reasonable to believe that the nonspecific binding signals can be reduced significantly if highly specific probe−target systems are investigated.

The gold nanorods were stabilized in the solution by CTAB capping on the {1,1,0}/{1,0,0} side faces with a biofunctionalization layer only along the {1,1,1} sides faces. Since the CTAB capping is physisorbed and less robust, CTAB molecules could leave the rod surface and re-enter the solution, especially when there is no CTAB in the solution. It has been noticed in our work as well as from others[29] that if nanorods were centrifuged and resuspended in water, centrifugation can only be conducted twice without losing the integrity of the rods. A third time centrifugation resulted in a significant loss of the CTAB capping and the formation of nanorod aggregates. Hence, resuspension of the nanorods in 0.005 M CTAB solution was necessary after each centrifugation in this study. The gold colloids thus produced remained stable even after five cycles of centrifugation−resuspension. At such low concentrations, CTAB only caused a minor denaturation of the antibodies and no significant dissociation of the antibody−antigen binding[30] was observed.

## CONCLUSION

The wavelength dependence of the longitudinal plasmon peaks on the aspect ratio of gold nanorods and the corresponding change in the refractive indexes in the immediate vicinity makes them extremely sensitive reporters of molecular binding events with excellent multiplexing capability. In this study, we have demonstrated for the first time that the exquisite optical properties of gold nanorods could be utilized to develop simple and sensitive lab-in-a-tube biosensors for multiplex detection of biological targets. It is shown that optical signals observed are due to the response of single rods to target binding events and not due to particle aggregates. The concept and methodology developed in this study can serve as the basis for developing new multiplex assays for the detection of molecular binding events for medical and biosecurity applications.

## ACKNOWLEDGMENT

The authors thank Dr. Robinson from Purdue University for providing sheep IgG and rabbit anti-sheep IgGs. The USDA challenge grant is acknowledged for partial funding of this work. The work was conducted at the Physiological Sensing Facility in Bindley Biosciences Center.

## SUPPORTING INFORMATION AVAILABLE

Additional information as noted in text. This material is available free of charge via the Internet at http://pubs.acs.org.

Received for review September 14, 2006. Accepted November 2, 2006.

AC061730D

(29) Takahashi, H.; Niidome, Y.; Niidome, T.; Kaneko, K.; Kawasaki, H.; Yamada, S. *Langmuir* **2006**, *22*, 2−5.

(30) Kandimalla, V. B.; Neeta, N. S.; Karanth, N. G.; Thakur, M. S.; Roshini, K. R.; Rani, B. E.; Pasha, A.; Karanth, N. G. *Biosens. Bioelectron.* **2004**, *20*, 903−906.